Supplementary materials:

Simultaneous design of non-Newtonian lubricant material and surface texture using surrogate-based multiobjective optimization

Yong Hoon Lee · Jonathon K. Schuh · Randy H. Ewoldt · James T. Allison
University of Illinois at Urbana-Champaign, Urbana, IL 61801, USA

1 Derivation CEF-Reynolds Equation

We use the CEF model in the incompressible Cauchy-Momentum equations (Bird et al. 1987; Owens and Phillips 2002),

$$\nabla \cdot \underline{u} = 0 \tag{1a}$$

$$\rho\left(\frac{\partial \underline{u}}{\partial t} + [\underline{u}\cdot\nabla]\,\underline{u}\right) = -\nabla p + \nabla\cdot\underline{\underline{\tau}} \tag{1b}$$

$$\underline{\underline{\tau}} = \eta\left(\dot{\gamma}\right)\underline{\underline{\gamma}}_{(1)} - \frac{1}{2}\Psi_1\left(\dot{\gamma}\right)\underline{\underline{\gamma}}_{(2)} + \Psi_2\left(\dot{\gamma}\right)\left[\underline{\underline{\gamma}}_{(1)}\cdot\underline{\underline{\gamma}}_{(1)}\right], \tag{1c}$$

where the $\underline{u}$ is the velocity vector, p is the pressure, and ρ is the fluid density, the gradient and divergence operators are appropriate for cylindrical coordinates, and the coordinate system is defined in Fig. 1.

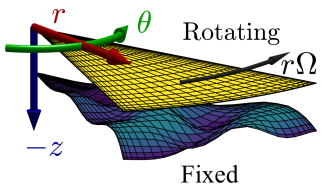

Fig. 1 Periodic cell of textured surface in cylindrical coordinates. The coordinate system and directions of motion are defined as shown.

We can simplify the governing equations in the thin film limit by assuming:

1. $h(r,\theta)/R \to 0$; thin film approximation to neglect velocity gradients in the flow direction.
2. The shear rate is
$$\dot{\gamma}\left(r,\theta\right) \equiv \sqrt{\frac{1}{2}\underline{\underline{\gamma}}_1 : \underline{\underline{\gamma}}_1} \approx \frac{r\Omega}{h\left(r,\theta\right)}, \tag{2}$$
which is independent of z, where Ω is the angular velocity of the flat plate.
3. $\Psi_2 = 0$, so that $\tau_{zz} = 0$.

Under these assumptions, the incompressible Cauchy momentum equations simplify to

$$\frac{1}{r}\frac{\partial}{\partial r}\left(ru_r\right)+\frac{1}{r}\frac{\partial u_\theta}{\partial \theta}+\frac{\partial u_z}{\partial z}=0 \tag{3a}$$

$$-\frac{\partial p}{\partial r}+\eta\left(\dot{\gamma}\right)\frac{\partial^2 u_r}{\partial z^2}+\frac{\Psi_1\left(\dot{\gamma}\right)}{r}\left[\left(\frac{\partial u_r}{\partial z}\right)^2-\left(\frac{\partial u_\theta}{\partial z}\right)^2\right]+\rho\frac{u_\theta^2}{r}=0 \tag{3b}$$

$$-\frac{1}{r}\frac{\partial p}{\partial \theta}+\eta\left(\dot{\gamma}\right)\frac{\partial^2 u_\theta}{\partial z^2}+\frac{2\Psi_1\left(\dot{\gamma}\right)}{r}\left[\left(\frac{\partial u_r}{\partial z}\right)\left(\frac{\partial u_\theta}{\partial z}\right)\right]-\rho\frac{u_r u_\theta}{r}=0 \tag{3c}$$

$$-\frac{\partial p}{\partial z}=0, \tag{3d}$$

with boundary conditions on the velocity field

$$u_r\left(z=-h\left(r,\theta\right)\right)=u_r\left(z=0\right)=0 \tag{4a}$$

$$u_\theta\left(z=-h\left(r,\theta\right)\right)=0,\ u_\theta\left(z=0\right)=r\Omega \tag{4b}$$

$$u_z\left(z=-h\left(r,\theta\right)\right)=u_z\left(z=0\right)=0 \tag{4c}$$

to satisfy the no slip and no penetration condtions, where u_r, u_θ, and u_z are the velocities in the r, θ, and z directions respectively. The resulting simplified Cauchy momentum equations are a set of coupled, non-linear, second order partial differential equations for the velocity.

1.1 Perturbation Solution

Because the governing equations are a set of coupled, non-linear partial differential equations, we choose to solve for the velocity and pressure fields using a regular perturbation expansion in both the Re_h and De for both the velocity and the pressure (Tichy and Chen 1985; Pinkus and Sternlicht 1961; Tichy 1996). We use the non-dimensional variables

$$r^*=\frac{r}{R} \tag{5a}$$

$$z^*=\frac{z}{h_0} \tag{5b}$$

$$u_r^*=\frac{u_r}{R\Omega} \tag{5c}$$

$$u_\theta^*=\frac{u_\theta}{R\Omega} \tag{5d}$$

$$u_z^*=\frac{u_z}{R\Omega\left(\frac{h_0}{R}\right)} \tag{5e}$$

$$\eta^*=\frac{\eta\left(\dot{\gamma}\right)}{\eta_0} \tag{5f}$$

$$\Psi_1^*=\frac{\Psi_1\left(\dot{\gamma}\right)}{\Psi_{10}} \tag{5g}$$

$$p^*=\frac{p}{\eta_0\Omega\left(\frac{R}{h_0}\right)^2} \tag{5h}$$

where R is the outer radius of the textured disk, h_0 is the maximum gap height, η_0 is the shear shear viscosity, and Ψ_{10} is the zero shear normal stress difference coefficient.

Substituting the non-dimensional variables into the governing equations gives

$$\frac{1}{r^*}\frac{\partial}{\partial r}\left(r^* u_r^*\right) + \frac{1}{r^*}\frac{\partial u_\theta^*}{\partial \theta} + \frac{\partial u_z^*}{\partial z^*} = 0 \tag{6a}$$

$$-\frac{\partial p^*}{\partial r^*} + \eta^* \frac{\partial^2 u_r^*}{\partial {z^*}^2} + \mathrm{De}\frac{\Psi_1^*}{r^*}\left[\left(\frac{\partial u_r^*}{\partial z^*}\right)^2 - \left(\frac{\partial u_\theta^*}{\partial z^*}\right)^2\right] + \mathrm{Re}_h \frac{{u_\theta^*}^2}{r^*} = 0 \tag{6b}$$

$$-\frac{1}{r^*}\frac{\partial p^*}{\partial \theta} + \eta^* \frac{\partial^2 u_\theta^*}{\partial {z^*}^2} + \mathrm{De}\frac{2\Psi_1^*}{r^*}\left[\left(\frac{\partial u_r^*}{\partial z^*}\right)\left(\frac{\partial u_\theta^*}{\partial z^*}\right)\right] - \mathrm{Re}_h \frac{u_r^* u_\theta^*}{r^*} = 0 \tag{6c}$$

$$-\frac{\partial p^*}{\partial z^*} = 0 \tag{6d}$$

where we have defined the Reynolds number as $\mathrm{Re}_h \equiv \frac{\rho \Omega h_0^2}{\eta_0}$ and the Deborah number as $\mathrm{De} \equiv \frac{\Psi_{10}\Omega}{\eta_0}$.

We expand the velocity and pressure fields using a regular perturbation expansion in both the Re_h and De (Tichy and Chen 1985; Pinkus and Sternlicht 1961; Tichy 1996),

$$u_r^* = u_{r_0}^* + \mathrm{Re}_h u_{r_I}^* + \mathrm{De} u_{r_E}^* + O\left(\mathrm{Re}_h^2, \mathrm{De}^2\right) \tag{7a}$$

$$u_\theta^* = u_{\theta_0}^* + \mathrm{Re}_h u_{\theta_I}^* + \mathrm{De} u_{\theta_E}^* + O\left(\mathrm{Re}_h^2, \mathrm{De}^2\right) \tag{7b}$$

$$u_z^* = u_{z_0}^* + \mathrm{Re}_h u_{z_I}^* + \mathrm{De} u_{z_E}^* + O\left(\mathrm{Re}_h^2, \mathrm{De}^2\right) \tag{7c}$$

$$p^* = p_0^* + \mathrm{Re}_h p_I^* + \mathrm{De} p_E^* + O\left(\mathrm{Re}_h^2, \mathrm{De}^2\right). \tag{7d}$$

We expand in this manner because in the limit that both the Re_h and De tend to 0, we should recover the governing equations for the traditional Reynolds equation (Reynolds 1886; Schuh et al. 2017).

After substituting the expansions into the governing equations and collecting the same order terms, we obtain the following non-dimensional equations:

0th Order Terms

$$\frac{1}{r^*}\frac{\partial}{\partial r}\left(r^* u_{r_0}^*\right) + \frac{1}{r^*}\frac{\partial u_{\theta_0}^*}{\partial \theta} + \frac{\partial u_{z_0}^*}{\partial z^*} = 0 \tag{8a}$$

$$\eta^* \frac{\partial^2 u_{r_0}^*}{\partial {z^*}^2} - \frac{\partial p_0^*}{\partial r^*} = 0 \tag{8b}$$

$$\eta^* \frac{\partial^2 u_{\theta_0}^*}{\partial {z^*}^2} - \frac{1}{r^*}\frac{\partial p_0^*}{\partial \theta} = 0 \tag{8c}$$

$$\frac{\partial p_0^*}{\partial z^*} = 0 \tag{8d}$$

Order Re_h Terms

$$\frac{1}{r^*}\frac{\partial}{\partial r}\left(r^* u_{r_I}^*\right) + \frac{1}{r^*}\frac{\partial u_{\theta_I}^*}{\partial \theta} + \frac{\partial u_{z_I}^*}{\partial z^*} = 0 \tag{9a}$$

$$\eta^* \frac{\partial^2 u_{r_I}^*}{\partial {z^*}^2} - \frac{\partial p_I^*}{\partial r^*} + \frac{{u_{\theta_0}^*}^2}{r^*} = 0 \tag{9b}$$

$$\eta^* \frac{\partial^2 u^*_{\theta_I}}{\partial {z^*}^2} - \frac{1}{r^*}\frac{\partial p^*_I}{\partial \theta} - \frac{u^*_{r_0} u^*_{\theta_0}}{r^*} = 0 \tag{9c}$$

$$\frac{\partial p^*_I}{\partial z^*} = 0 \tag{9d}$$

Order De Terms

$$\frac{1}{r^*}\frac{\partial}{\partial r}\left(r^* u^*_{r_E}\right) + \frac{1}{r^*}\frac{\partial u^*_{\theta_E}}{\partial \theta} + \frac{\partial u^*_{z_E}}{\partial z^*} = 0 \tag{10a}$$

$$\eta^* \frac{\partial^2 u^*_{r_E}}{\partial {z^*}^2} - \frac{\partial p^*_E}{\partial r^*} + \frac{\Psi^*_1}{r^*}\left[\left(\frac{\partial u^*_{r_0}}{\partial z^*}\right)^2 - \left(\frac{\partial u^*_{\theta_0}}{\partial z^*}\right)^2\right] = 0 \tag{10b}$$

$$\eta^* \frac{\partial^2 u^*_{\theta_E}}{\partial {z^*}^2} - \frac{1}{r^*}\frac{\partial p^*_E}{\partial \theta} + \frac{2\Psi^*_1}{r^*}\left[\left(\frac{\partial u^*_{r_0}}{\partial z^*}\right)\left(\frac{\partial u^*_{\theta_0}}{\partial z^*}\right)\right] = 0 \tag{10c}$$

$$\frac{\partial p^*_E}{\partial z^*} = 0 \tag{10d}$$

To simplify the total number of governing equations, we combine the corresponding equations for the order Re_h and order De terms, since both equations are linear in the variables of interest and both must satisfy the incompressibility constraint. After performing the superposition, we introduce new variables, defined as

$$u^*_{r_1} = u^*_{r_I} + u^*_{r_E} \tag{11a}$$

$$u^*_{\theta_1} = u^*_{\theta_I} + u^*_{\theta_E} \tag{11b}$$

$$u^*_{z_1} = u^*_{z_I} + u^*_{z_E} \tag{11c}$$

$$p^*_1 = p^*_I + p^*_E \tag{11d}$$

so that the resulting equations are

$$\frac{1}{r^*}\frac{\partial}{\partial r}\left(r^* u^*_{r_1}\right) + \frac{1}{r^*}\frac{\partial u^*_{\theta_1}}{\partial \theta} + \frac{\partial u^*_{z_1}}{\partial z^*} = 0 \tag{12a}$$

$$\eta^* \frac{\partial^2 u^*_{r_1}}{\partial {z^*}^2} - \frac{\partial p^*_1}{\partial r^*} + \frac{\Psi^*_1}{r^*}\left[\left(\frac{\partial u^*_{r_0}}{\partial z^*}\right)^2 - \left(\frac{\partial u^*_{\theta_0}}{\partial z^*}\right)^2\right] + \frac{{u^*_{\theta_0}}^2}{r^*} = 0 \tag{12b}$$

$$\eta^* \frac{\partial^2 u^*_{\theta_1}}{\partial {z^*}^2} - \frac{1}{r^*}\frac{\partial p^*_1}{\partial \theta} + \frac{2\Psi^*_1}{r^*}\left[\left(\frac{\partial u^*_{r_0}}{\partial z^*}\right)\left(\frac{\partial u^*_{\theta_0}}{\partial z^*}\right)\right] - \frac{u^*_{r_0} u^*_{\theta_0}}{r^*} = 0 \tag{12c}$$

$$\frac{\partial p_1}{\partial z^*} = 0. \tag{12d}$$

In dimensional form, this gives us the final set of governing equations with appropriate boundary conditions. Once the 0th order terms are known, the 1st order terms can be obtained.

0th Order

$$\frac{1}{r}\frac{\partial}{\partial r}\left(r u_{r_0}\right) + \frac{1}{r}\frac{\partial u_{\theta_0}}{\partial \theta} + \frac{\partial u_{z_0}}{\partial z} = 0 \tag{13a}$$

$$\eta\left(\dot{\gamma}\right)\frac{\partial^2 u_{r_0}}{\partial z^2} - \frac{\partial p_0}{\partial r} = 0 \tag{13b}$$

$$\eta\left(\dot{\gamma}\right)\frac{\partial^2 u_{\theta_0}}{\partial z^2}-\frac{1}{r}\frac{\partial p_0}{\partial \theta}=0 \tag{13c}$$

$$\frac{\partial p_0}{\partial z}=0 \tag{13d}$$

$$u_{r_0}\left(z=-h\left(r,\theta\right)\right)=u_{r_0}\left(z=0\right)=0 \tag{13e}$$

$$u_{\theta_0}\left(z=-h\left(r,\theta\right)\right)=0,\ u_{\theta_0}\left(z=0\right)=r\Omega \tag{13f}$$

$$u_{z_0}\left(z=-h\left(r,\theta\right)\right)=u_{z_0}\left(z=0\right)=0 \tag{13g}$$

1st Order

$$\frac{1}{r}\frac{\partial}{\partial r}\left(ru_{r_1}\right)+\frac{1}{r}\frac{\partial u_{\theta_1}}{\partial \theta}+\frac{\partial u_{z_1}}{\partial z}=0 \tag{14a}$$

$$\eta\left(\dot{\gamma}\right)\frac{\partial^2 u_{r_1}}{\partial z^2}-\frac{\partial p_1}{\partial r}+\frac{\Psi_1\left(\dot{\gamma}\right)}{r}\left[\left(\frac{\partial u_{r_0}}{\partial z}\right)^2-\left(\frac{\partial u_{\theta_0}}{\partial z}\right)^2\right]+\rho\frac{u_{\theta_0}^2}{r}=0 \tag{14b}$$

$$\eta\left(\dot{\gamma}\right)\frac{\partial^2 u_{\theta_1}}{\partial z^2}-\frac{1}{r}\frac{\partial p_1}{\partial \theta}+\frac{2\Psi_1\left(\dot{\gamma}\right)}{r}\left[\left(\frac{\partial u_{r_0}}{\partial z}\right)\left(\frac{\partial u_{\theta_0}}{\partial z}\right)\right]-\rho\frac{u_{r_0}u_{\theta_0}}{r}=0 \tag{14c}$$

$$\frac{\partial p_1}{\partial z}=0 \tag{14d}$$

$$u_{r_1}\left(z=-h\left(r,\theta\right)\right)=u_{r_1}\left(z=0\right)=0 \tag{14e}$$

$$u_{\theta_1}\left(z=-h\left(r,\theta\right)\right)=u_{\theta_1}\left(z=0\right)=0 \tag{14f}$$

$$u_{z_1}\left(z=-h\left(r,\theta\right)\right)=u_{z_1}\left(z=0\right)=0 \tag{14g}$$

1.2 CEF-Reynolds Equation

We solve the governing equations given in the boxes above in the same manner as the tradition Reynolds equation (Schuh et al. 2017; Reynolds 1886). The steps are:

1. Obtain the velocities in the r and θ direction in terms of the unknown pressure field and the boundary conditions.
2. Substitute the obtained velocities into the incompressibility equation.
3. Integrate over the z direction and use Leibniz's rule for integrating the derivatives in the r and θ direction.

Using these steps, we eventually obtain two equations for the unknown pressure fields p_0 and p_1, given as

0th Order

$$\frac{1}{r}\frac{\partial}{\partial r}\left(\frac{rh^3}{12\eta}\frac{\partial p_0}{\partial r}\right)+\frac{1}{r}\frac{\partial}{\partial \theta}\left(\frac{h^3}{12\eta r}\frac{\partial p_0}{\partial \theta}\right)=\frac{1}{r}\frac{\partial}{\partial \theta}\left(\frac{r\Omega h}{2}\right) \tag{15}$$

1st Order

$$\frac{1}{r}\frac{\partial}{\partial r}\left(\frac{rh^3}{12\eta}\frac{\partial p_1}{\partial r}\right)+\frac{1}{r}\frac{\partial}{\partial \theta}\left(\frac{h^3}{12\eta r}\frac{\partial p_1}{\partial \theta}\right)=\frac{1}{r}\frac{\partial}{\partial r}\left(rG_r\right)+\frac{1}{r}\frac{\partial}{\partial \theta}\left(G_\theta\right) \tag{16a}$$

$$G_r=\frac{r\Omega h}{40}\left(\frac{\rho\Omega h^2}{\eta}\right)B_r+\frac{r\Omega h}{12}\left(\frac{\Psi_1\Omega}{\eta}\right)A_r \tag{16b}$$

$$B_r=1-\frac{1}{3}\left(\frac{1}{\eta\Omega}\frac{\partial p_0}{\partial \theta}\left(\frac{h}{r}\right)^2\right)+\frac{1}{28}\left(\frac{1}{\eta\Omega}\frac{\partial p_0}{\partial \theta}\left(\frac{h}{r}\right)^2\right)^2 \tag{16c}$$

$$A_r=-1-\frac{1}{20}\left(\frac{1}{\eta\Omega}\frac{\partial p_0}{\partial \theta}\left(\frac{h}{r}\right)^2\right)^2+\frac{1}{20}\left(\frac{1}{\eta\Omega}r\frac{\partial p_0}{\partial r}\left(\frac{h}{r}\right)^2\right)^2 \tag{16d}$$

$$G_\theta=\frac{r\Omega h}{240}\left(\frac{\rho\Omega h^2}{\eta}\right)B_\theta+\frac{r\Omega h}{120}\left(\frac{\Psi_1\Omega}{\eta}\right)A_\theta \tag{16e}$$

$$B_\theta=\left(\frac{1}{\eta\Omega}r\frac{\partial p_0}{\partial r}\left(\frac{h}{r}\right)^2\right)-\frac{3}{14}\left(\frac{1}{(\eta\Omega)^2}r\frac{\partial p_0}{\partial r}\frac{\partial p_0}{\partial \theta}\left(\frac{h}{r}\right)^4\right) \tag{16f}$$

$$A_\theta=\left(\frac{1}{(\eta\Omega)^2}r\frac{\partial p_0}{\partial r}\frac{\partial p_0}{\partial \theta}\left(\frac{h}{r}\right)^4\right) \tag{16g}$$

Equation 15 resembles the traditional form of the Reynolds equation in cylindrical coordinates (Schuh et al. 2017; Beschorner et al. 2008), and includes shear thinning. Equation 16a also resembles the traditional Reynolds equation, and the right hand side depends on the local Reynolds number Re_h and the local relation of elasticity to viscosity, which can be interpreted as a local Deborah number, De.

Once Equations 15 and 16a are solved (with suitable boundary conditions), the velocity field can be obtained. The obtained pressure and velocity fields can then be used to calculate the normal force and torque on the moving flat plate.

2 Support Vector Domain Description (SVDD)

We constructed the Gaussian kernel-based SVDD (Tax and Duin 1999) using a maximization problem given as:

$$\underset{\underline{0}\leq\underline{\beta}\leq\underline{C}}{\text{maximize}} \quad W\left(\underline{\beta}\right)=\sum_i \beta_i K_G\left(\underline{x}_i,\underline{x}_i\right)-\sum_{i,j}\beta_i\beta_j K_G\left(\underline{x}_i,\underline{x}_j\right) \tag{17}$$

where $\underline{C}$ is a vector of constant C, which is a parameter value that constrains the Lagrange multiplier $\underline{\beta}$ and is used to detect the outliers of the described domain. Using the Gaussian kernel function (or any other kernel function that satisfies Mercer's theorem (Mercer 1909)) allows the implicit mapping of objects $\underline{x}$ to some feature space, which allows the encapsulating hypersphere to tightly describe the region of the clouds of objects. The Gaussian kernel is defined as:

$$K_G\left(\underline{x}_i,\underline{x}_j\right)=\exp\left(-q\left|\left|\underline{x}_i-\underline{x}_j\right|\right|^2\right), \tag{18}$$

where $q \geq 0$ is the width parameter, which quantifies how tightly-encapsulate the boundaries of the point clouds will be. Testing if any arbitrary point $\underline{z}$ is inside the encapsulated domain can be performed using the computation of distance from the center of the featured space constructed from Eq. 17 given as:

$$R^2\left(\underline{z}\right) = K_G\left(\underline{z},\underline{z}\right) - 2\sum_i \beta_i K_G\left(\underline{z},\underline{x}_i\right) + \sum_{i,j} \beta_i \beta_j K_G\left(\underline{x}_i,\underline{x}_j\right) \tag{19}$$

and the arbitrary point $\underline{z}$ is inside the described boundary if

$$R^2\left(\underline{x}\right) - R^2\left(\underline{z}\right) = K_G\left(\underline{x},\underline{x}\right) - K_G\left(\underline{z},\underline{z}\right) + 2\sum_i \beta_i \left(K_G\left(\underline{z},\underline{x}_i\right) - K_G\left(\underline{x}_i,\underline{x}_i\right)\right) \geq 0 \tag{20}$$

where $\underline{x}$ is a bounding point, which is called a support vector.

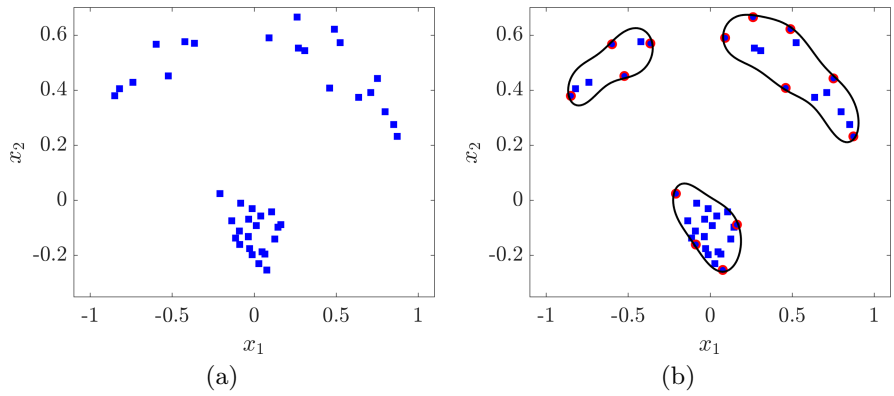

Fig. 2 A test case showing how the SVDD algorithm describes boundaries of the data point clouds. (a) shows an artificial data set in 2D space, and (b) shows the support vectors (data points with red circles) and the domain encapsulating the data point clouds (black curved lines)

Fig. 2 shows a test case with an artificial data set in two-dimensional space. A detailed description of the SVDD derivation can be found in Tax and Duin (1999), and more test cases using the SVDD based on the Gaussian kernel are demonstrated in Malak and Paredis (2010).

3 Experimental Validation of Fluid and Texture Solvers

The thin-film Reynolds equation with CEF fluid (CEF-Reynolds) and the full 3-D momentum equation with Giesekus fluid (Giesekus-3D) solvers are validated against steady shear experiments for varying concentrations of polyisobutylene (PIB) in S6 base mineral oil using a cone-and-plate rheometer geometry of Θ=1.011° and R=0.02 m, where Θ and R denote the cone angle and the radius, respectively. Since we use the same parameterizations for CEF and Giesekus fluids, we performed a least-square fitting for the two-mode Giesekus fluid using the experimental data for six different concentrations: 0.05, 0.1, 0.18, 0.357, 0.5, and 0.76 wt% of

PIB solution in a Newtonian mineral base oil (trade name: S6 Newtonian viscosity standard, Cannon Instrument Company, η_s=9.624 mPa-s at 20°C). Using fitted parameters, the cone-and-plate geometry is numerically modeled for both CEF-Reynolds and Giesekus-3D solvers and simulated for the six fluid concentrations and the entire angular velocity range that covers the shear rate range of obtained experimental data.

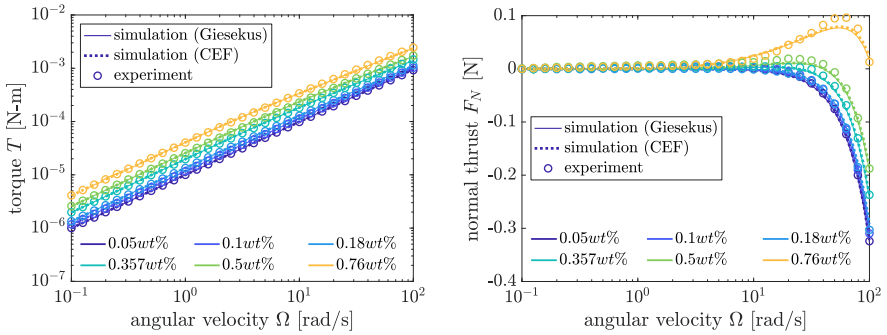

Fig. 3 Comparison of raw torque T and raw normal force F_N data from experiments using a cone-and-plate rheometer geometry and simulations using CEF-Reynolds and Giesekus-3D solvers. (a) Torque T, and (b) Normal force F_N.

The comparison of the raw torque T and the raw normal force (thrust) F_N experimental data (circles) to simulation results (dotted line: CEF-Reynolds, solid line: Giesekus-3D) is shown in Fig. 3. Good agreement is seen between the experiments and the simulations for the cone-and-plate rheometer geometry with a steady shear condition.

4 Solver Parameter Sensitivity Analysis

We analyzed ranges of solutions affected by mechanical and fluid parameter uncertainties for our numerical solvers using a differential sensitivity analysis method. Mechanical parameters include geometrical and operating parameters, including the radius of the parallel discs, minimum controlled gap height between discs, and angular velocity of the rotating disc. Fluid parameters include operating temperature, which affects solvent viscosity. Design variables in the fluid parameters, such as polymeric viscosity, relaxation time, and the mobility factor of design target viscoelastic fluid, are not assessed here because they are design targets rather than measured properties in this study.

The radius of the discs (R_o) as well as the textured disc can be very precisely manufactured for the tribo-rheometric experiments. However, to see the effect of radius changes, we set a deviation of ± 50 μm. The nominal gap height ($h_{\min}$), which serves as a minimum gap height between the discs in this study, can affect the apparent viscosity of the system directly. According to Schuh and Ewoldt (2016), the maximum gap offset between true and apparent gap values is 19 μm during

the gap zeroing procedure in the experiment. Thus, we set a deviation of +19 μm for the minimum gap height. The measured value of the solvent viscosity (η_s) is 9.624 mPa-s, which is less than 5% lower than the specification value of 10 mPa-s; thus, we set a deviation of ±5% for the solvent viscosity. The measured density of the solvent (ρ_s) is 873.4 kg/m^3, which is 0.5% lower than the specification value of 878 kg/m^3; thus, we set a deviation of ±1% for the solvent density that covers this difference with enough margin.

Tables 1 and 2 show changes in the objective functions (f_1: power input, f_2: normal force) when each parameter variable deviates specified amount for CEF-Reynolds and Giesekus-3D solvers respectively. We performed this differential sensitivity analysis on 6 select designs for each case; thus, the deviations in the objective functions have mean values and standard deviation values (with ± sign) in their table entries.

Table 1 Result of differential sensitivity analysis for the CEF-Reynolds solver parameters

variable	deviation	deviations in f_1 [%]	deviations in f_2 [%]
$R_o = 20$ mm	-50 μm	-0.941 ± 0.031	-0.924 ± 0.035
	$+50$ μm	$+0.948\pm0.032$	$+0.931\pm0.035$
$h_{\min} = 269$ μm	$+19$ μm	-4.164 ± 0.492	-11.398 ± 0.390
$\Omega = 10$ rad/s	-1%	-1.772 ± 0.125	-0.927 ± 0.159
	$+1$%	$+1.785\pm0.129$	$+0.928\pm0.160$
$\eta_s = 9.624$ mPa-s	-5%	-2.481 ± 1.619	-2.024 ± 1.368
	$+5$%	$+2.481\pm1.619$	$+2.023\pm1.368$
$\rho_s = 873.4$ kg/m^3	-1%	$+7.6\text{e-}6\pm5.8\text{e-}6$	-0.048 ± 0.083
	$+1$%	$-7.6\text{e-}6\pm5.8\text{e-}6$	$+0.048\pm0.083$

Table 2 Result of differential sensitivity analysis for the Giesekus-3D solver parameters

variable	deviation	deviations in f_1 [%]	deviations in f_2 [%]
$R_o = 20$ mm	-50 μm	-0.860 ± 0.265	-0.458 ± 1.314
	$+50$ μm	$+0.978\pm0.018$	$+1.005\pm0.020$
$h_{\min} = 269$ μm	$+19$ μm	-4.599 ± 0.855	-10.100 ± 1.574
$\Omega = 10$ rad/s	-1%	-1.787 ± 0.270	-0.501 ± 1.329
	$+1$%	$+1.912\pm0.059$	$+1.047\pm0.077$
$\eta_s = 9.624$ mPa-s	-5%	-2.770 ± 1.662	-1.869 ± 0.887
	$+5$%	$+2.570\pm1.684$	$+2.479\pm2.178$
$\rho_s = 873.4$ kg/m^3	-1%	$+0.106\pm0.271$	$+0.442\pm1.343$
	$+1$%	-0.052 ± 0.128	$+0.316\pm0.474$

References

Beschorner KE, Higgs III CF, Lovell MR (2008) Derivation of Reynolds equation in cylindrical coordinates applicable to pin-on-disk and CMP. In: Proceedings of the STLE/ASME International Joint Tribology Conference, Miami, FL, IJTC2008-71245, pp 399–401, DOI 10.1115/IJTC2008-71245

Bird RB, Armstrong RC, Hassager O (1987) Dynamics of Polymeric Liquids, vol 1 Fluid Mechanics, 2nd edn. Wiley, New York, NY, ISBN 978-0-471-80245-7

Malak RJ Jr, Paredis CJJ (2010) Using support vector machines to formalize the valid input domain of predictive models in systems design problems. Journal of Mechanical Design 132(10):101001, DOI 10.1115/1.4002151

Mercer J (1909) Functions of positive and negative type, and their connection the theory of integral equations. Philosophical Transactions of the Royal Society of London A: Mathematical, Physical and Engineering Sciences 209(441-458):415–446, DOI 10.1098/rsta.1909.0016

Owens RG, Phillips TN (2002) Computational Rheology. Imperial College Press, London, UK, ISBN 978-1-86094-186-3

Pinkus O, Sternlicht B (1961) Theory of Hydrodynamic Lubrication. McGraw-Hill, New York, NY

Reynolds O (1886) On the theory of lubrication and its application to Mr. Beauchamp Tower's experiments, including an experimental determination of the viscosity of olive oil. Philosophical Transactions of the Royal Society of London 177:157–234, DOI 10.1098/rspl.1886.0021

Schuh JK, Ewoldt RH (2016) Asymmetric surface textures decrease friction with Newtonian fluids in full film lubricated sliding contact. Tribology International 97:490–498, DOI 10.1016/j.triboint.2016.01.016

Schuh JK, Lee YH, Allison JT, Ewoldt RH (2017) Design-driven modeling of surface-textured full-film lubricated sliding: Validation and rationale of nonstandard thrust observations. Tribology Letters 65(2):35–1–17, DOI 10.1007/s11249-017-0818-8

Tax DM, Duin RP (1999) Support vector domain description. Pattern Recognition Letters 20(11-13):1191–1199, DOI 10.1016/S0167-8655(99)00087-2

Tichy JA (1996) Non-Newtonian lubrication with the convected Maxwell model. Journal of Tribology 118(2):344–348, DOI 10.1115/1.2831307

Tichy JA, Chen SH (1985) Plane slider bearing load due to fluid inertia–experiment and theory. Journal of Tribology 107(1):32–38, DOI 10.1115/1.3260999